

## Synthesis and Photocatalytic Activity of TiO<sub>2</sub>/BiVO<sub>4</sub> Layered Films under Visible Light Irradiation

Xuan Li<sup>\*\*\*</sup>, Zhuo Zhang<sup>\*</sup>, Feng-Jun Zhang<sup>\*\*\*†</sup>, Jin Liu<sup>\*\*\*</sup>, Jie Ye<sup>\*\*</sup>, and Won-Chun Oh<sup>\*\*\*‡</sup>

<sup>\*</sup>Anhui Key Laboratory of Advanced Building Materials, Anhui Jianzhu University, Hefei Anhui 230022, P. R. China,

<sup>\*\*</sup>Key Laboratory of Functional Molecule Design and Interface Process, Anhui Jianzhu University, Hefei Anhui 230601, P. R. China

<sup>\*\*\*</sup>Department of Advanced Materials Science & Engineering, Hanseo University, Seosan 31962, Korea

(Received May 1, 2016; Revised August 6, 2016; Accepted October 7, 2016)

### ABSTRACT

TiO<sub>2</sub>/BiVO<sub>4</sub> layered films were prepared by sol-gel and spin coating methods. X-ray diffraction (XRD), scanning electron microscopy (SEM) and Uv-vis spectroscopy were used to investigate the crystal structure, morphology and ultraviolet-visible absorption of the TiO<sub>2</sub>/BiVO<sub>4</sub> films. The photocatalytic activity of the prepared films was inspected according to the degradation of methylene blue. The results show that the prepared films present a net chain structure; the absorption band edge had obvious red shift. The degradation of the methylene blue solution was about 80% after 300 mins using TiO<sub>2</sub>/BiVO<sub>4</sub> layered films under visible light, which was stronger than when using only pure TiO<sub>2</sub> film and BiVO<sub>4</sub> film.

**Key words :** Layered films, TiO<sub>2</sub>, BiVO<sub>4</sub>, Photocatalysis, Visible light

### 1. Introduction

Since the 20th century, the rapid development of human society, the humanities and science have had fruitful results, but subsequent problems related to resources and ecology have seen all countries scrambling to try to solve such problems. Solar energy, as a non-polluting and renewable source of energy, should not be ignored or wasted. Therefore, the priority is how to effect the efficient utilization and conversion of solar energy.<sup>1)</sup>

Since Honda-Fujishima<sup>2)</sup> discovered the phenomenon in which a TiO<sub>2</sub> semiconductor electrode performs catalytic decomposition of water, photocatalytic technology has attracted the attention of researchers, and this technology has provided us with an ideal method of energy utilization and control of environmental pollution. Photocatalytic technology is an advanced technology<sup>3)</sup> in which a catalyst uses photon energy to make many reactions that normally take place in harsh conditions respond in a mild environment. At present, the TiO<sub>2</sub> based photocatalyst has the advantages of energy saving, no pollution, low price and high efficiency for the degradation of organic pollutants, which has become a hot research field.<sup>4)</sup> However, TiO<sub>2</sub>, because of its band gap of 3.2 eV, can be induced to react only by ultraviolet irradiation,<sup>5)</sup>

and ultraviolet content in the solar spectrum is only around 3%, which limits practical applications in dealing with environmental problems.<sup>6)</sup> Therefore, the key is doping modification of a nanometer TiO<sub>2</sub> catalyst to improve the degree of visible light response, so as to improve the utilization rate of solar energy. Wang<sup>7)</sup> reported the amphiphathic of TiO<sub>2</sub> thin film in *Nature* in 1997, which article opened up a new direction in practical applications. The water contact angle of new preparation of TiO<sub>2</sub> thin film is about 15°, while the water contact angle can be infinitely close to 0° under ultraviolet light irradiation, which indicates super hydrophilicity.<sup>8)</sup>

Since Kudo reported the properties of BiVO<sub>4</sub> for water splitting under visible light for the first time, study in the field of photocatalysis has received wide attention.<sup>9)</sup> The compound BiVO<sub>4</sub> has three crystal types: monoclinic (s-m), tetragonal (s-t) phase, and a zirconia structure with a tetragonal (z-t) phase.<sup>10)</sup> Studies have shown that the forbidden band width of monoclinic scheelite is about 2.4 eV, which is the section that includes most of the visible light response and the strongest photocatalytic activity. However, the photocatalytic ability of pure BiVO<sub>4</sub> is not strong because of the weak adsorption ability and because the composite easily produces electrons and holes.<sup>11)</sup> Studies have shown that a composite of TiO<sub>2</sub> powders and BiVO<sub>4</sub> powder can effectively improve the photocatalytic ability.<sup>12-14)</sup>

Studies and reports of single TiO<sub>2</sub> thin films and BiVO<sub>4</sub> films have been numerous, but composites of two kinds of thin film have not yet been reported. We prepared TiO<sub>2</sub>/BiVO<sub>4</sub> layered film used the sol-gel process. X-ray diffraction (XRD), scanning electron microscopy (SEM) and Uv-Vis

<sup>†</sup>Corresponding author : Feng-Jun Zhang

E-mail : zhang-fengjun@hotmail.com

Tel : +86-551-6382-8262 Fax : +86-551-6382-8106

<sup>‡</sup>Corresponding author : Won-Chun Oh

E-mail : wc\_oh@hanseo.ac.kr

Tel : +82-41-660-1337 Fax : +82-41-688-3352

spectroscopy were used to investigate the film crystal structure, morphology and ultraviolet-visible absorption ability. At the same time, the photocatalytic activity of the film was inspected through the degradation of methylene blue.

## 2. Experimental Procedure

### 2.1. Preparation of $\text{TiO}_2$ thin film

Butyl titanate (13 ml) was dissolved in anhydrous ethanol (12 ml) and diethanolamine (5 ml); then, the mixed solution was stirred for 1h at room temperature. Next, we added deionized water (1.7 ml), anhydrous ethanol (34 ml) and HCl (0.13 ml) to the above solution and stirred it for 15 min to form a clear yellow liquid. After this, the liquid was aged for 24 hours and a sol formed.  $\text{TiO}_2$  thin films were prepared by spin coating method (speed 3000 r/min, rotated for 30 s) using the sol. The wet films were pre-annealed at  $100^\circ\text{C}$  for 2 min and we then repeated the above procedures to get different thicknesses of  $\text{TiO}_2$  thin film. Finally, the films were annealed at  $600^\circ\text{C}$  for 1h in the air (the heating rate was  $2^\circ\text{C}/\text{min}$ ).

### 2.2. Preparation of $\text{BiVO}_4$ thin film

0.01 mol  $\text{Bi}(\text{NO}_3)_3 \cdot 5\text{H}_2\text{O}$  and 0.01 mol  $\text{NH}_4\text{VO}_3$  were added to 0.01 mol citric acid and 30 ml 23.3%  $\text{HNO}_3$  solution; mixture was stirred evenly, and 7.5 ml acetic acid and 0.2 g PVP K30 were dissolved in the above solution; after this, the solution was stirred for 5h, and a blue sol formed. Citric acid and acetic acid were the chelating agent; PVP K30 was the film-promoter.  $\text{BiVO}_4$  thin films were prepared by spin coating method (speed of 3000 r/min, rotated for 30 s) using the sol. The wet films were pre-annealed at  $180^\circ\text{C}$  for 2 min and we then repeated the above procedures to get different thicknesses of the  $\text{BiVO}_4$  thin film. Finally, the films were annealed at  $400^\circ\text{C}$  for 5h in air (the heating rate was  $4^\circ\text{C}/\text{min}$ ).

### 2.3. Preparation of $\text{TiO}_2/\text{BiVO}_4$ thin film

$\text{BiVO}_4$  sol, which was made using the same preparation methods as those detailed in 2.2, was coated on the  $\text{TiO}_2$  thin film prepared used the methods in 2.1, which included using the spin coating method (3000 r/min, rotate 30 s). The wet films were pre-annealed at  $180^\circ\text{C}$  for 2 min and we then repeated the above procedures to get different thicknesses of the  $\text{TiO}_2/\text{BiVO}_4$  thin film. Finally, the films were annealed at  $400^\circ\text{C}$  for 5h in air (the heating rate was  $4^\circ\text{C}/\text{min}$ ).

### 2.4 Characterization

X-ray diffraction (XRD) patterns were obtained with a Bruker (Germany) D8 Advance (Cu radiation, tube voltage 40 kV, tube current 40 mA,  $0.22^\circ$  step size,  $0.4^\circ/\text{step}$  scanning speed, scanning range of  $10^\circ$ - $70^\circ$ ) device. SEM images were obtained with a JEOL JSM-7500F. We used the Shanghai UV-8000S series of ultraviolet spectrophotometer to measure the ultraviolet-visible absorption (scanning

wavelength range is 200-800 nm). Methylene blue was degraded with a CEL-HXF300 xenon lamp light source.

## 3. Results and Discussion

### 3.1. Phase analysis of the sample

Figure 1 shows the XRD of the  $\text{TiO}_2$  powders and the  $\text{TiO}_2$  thin film. It can be seen that (101), (004) and (200) peaks of the  $\text{TiO}_2$  powders were found at  $25.44^\circ$ ,  $38.1^\circ$  and  $48.02^\circ$ , respectively. The sample was pure anatase  $\text{TiO}_2$  with high purity. The (101) peak of the  $\text{TiO}_2$  thin film was found at  $25.44^\circ$ , which showed that the  $\text{TiO}_2$  thin film was anatase; another characteristic peak was overshadowed by the characteristic peak of the glass substrate.

Figure 2 shows the XRD of the  $\text{BiVO}_4$  powder and the  $\text{BiVO}_4$  thin film.  $\text{BiVO}_4$  powder was bright yellow at pH = 4;  $\text{BiVO}_4$  powder was khaki. The XRD images of the powders with different pH and  $\text{BiVO}_4$  thin films are shown in Fig. 4.1. T represents the tetragonal(s-t) phases; M represents the monoclinic phase. In contrast with the PDF CARDS, it can be found that the  $\text{BiVO}_4$  powder had tetragonal(s-t)

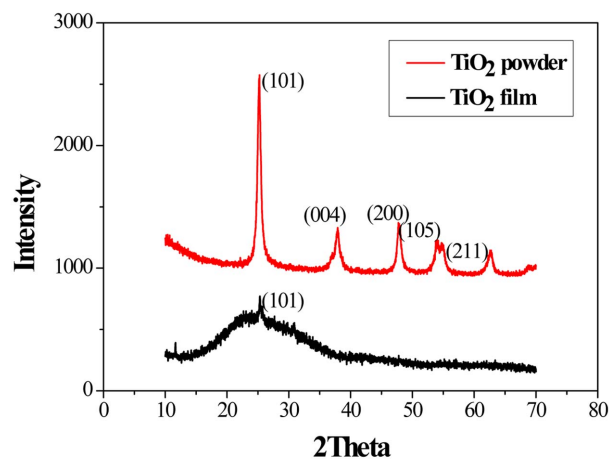


Fig. 1. XRD patterns of  $\text{TiO}_2$  powder and  $\text{TiO}_2$  thin film.

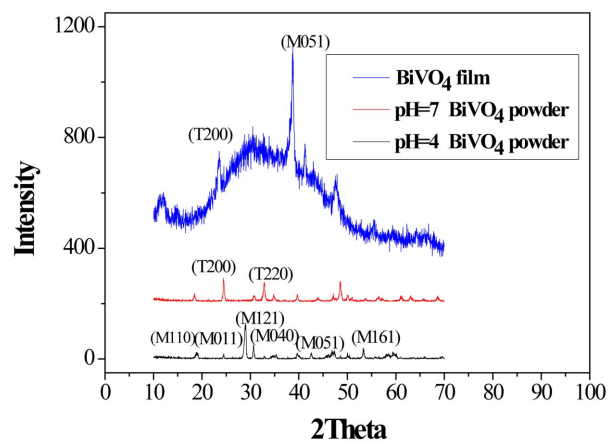


Fig. 2. XRD patterns of  $\text{BiVO}_4$  powder and  $\text{BiVO}_4$  film under different conditions.

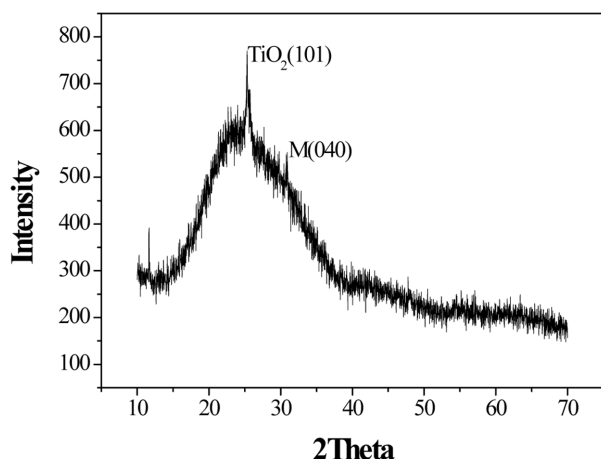


Fig. 3. XRD pattern of  $\text{TiO}_2/\text{BiVO}_4$  thin film.

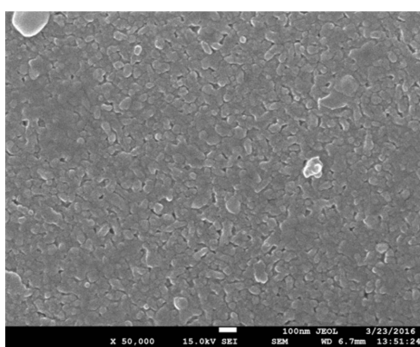


Fig. 4. SEM of T-11 film.

phases at  $\text{pH} = 7$ , while  $\text{BiVO}_4$  was in monoclinic phase at  $\text{pH} = 4$ . The color and crystal shape matching were consistent with those in the literature. T (200) and M (051) peaks were found in the XRD of the  $\text{BiVO}_4$  thin film; this image shows that the  $\text{BiVO}_4$  thin film was a mixture of monoclinic phase and tetragonal(s-t) phases.

Figure 3 shows the XRD of the  $\text{TiO}_2/\text{BiVO}_4$  layered film. The (101) characteristic peak of  $\text{TiO}_2$  was found at  $25^\circ$ , and the (040) characteristic peak of monoclinic phase  $\text{BiVO}_4$  was found at  $30.6^\circ$ ; this shows that the thin film contained anatase  $\text{TiO}_2$  and monoclinic phase  $\text{BiVO}_4$ , while other characteristic peaks were concealed by the peaks of the glass substrates.

### 3.2. Morphology analysis of the sample

Figure 4 shows the SEM results for the  $\text{TiO}_2$  thin film, in which the coating number was 11 (hereinafter referred to as the T-11 film). These results show that the T-11 film was uniform, with no cracking phenomenon. The size of the particles was about 40 nm; a few impurities were found on the surface. Fig. 5 shows the SEM results for the  $\text{BiVO}_4$  powder under different levels of pH. Fig. 5(a) shows the SEM results of the  $\text{BiVO}_4$  powder at  $\text{pH}=4$ ; it can be seen that the  $\text{BiVO}_4$  powder was spherical, had uniform dispersion, had no reunion phenomenon and that the size of the particles

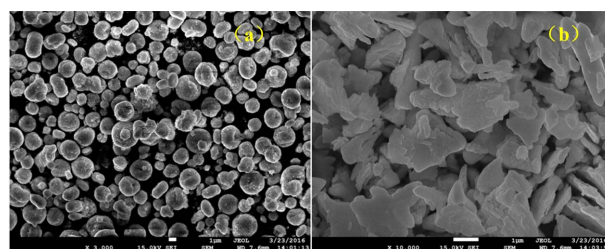


Fig. 5. SEM of  $\text{BiVO}_4$  powder under different pH.

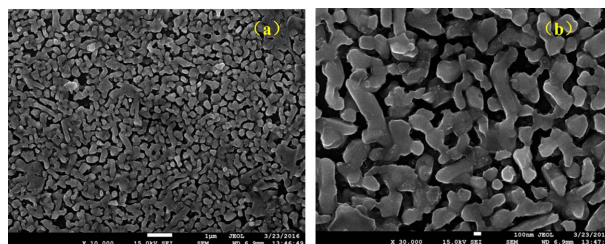


Fig. 6. SEM of B-3 film with different magnifications.

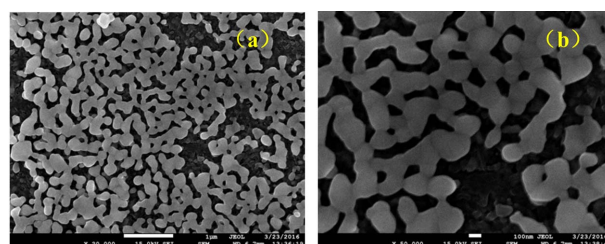


Fig. 7. SEM of  $\text{TiO}_2/\text{BiVO}_4$  film with different magnifications.

was about 1-2  $\mu\text{m}$ . Fig. 5(b) provides the SEM results of the  $\text{BiVO}_4$  powder at  $\text{pH} = 7$ ; it shows that the  $\text{BiVO}_4$  powder had a flowered layering; its thickness was about 0.1-0.5  $\mu\text{m}$ . Fig. 6 shows the SEM results of the  $\text{BiVO}_4$  thin film, in which the coating number was 3 (this is hereinafter referred to as the B-3 film). It can be seen that the B-3 film presented a network chain structure, which was uniform and showed no reunions. The width of the single chain was about 0.1  $\mu\text{m}$ ; the length was about 1  $\mu\text{m}$ . Fig. 7 shows the SEM results of the  $\text{TiO}_2/\text{BiVO}_4$  film with different levels of magnification. It can be seen from Fig. 7(a) that the dark part at the bottom was  $\text{TiO}_2$  thin film, the bright part was  $\text{BiVO}_4$  thin film, the top film was relatively uniform and there was a certain degree of fracturing. It can be seen from Fig. 7(b) that the  $\text{BiVO}_4$  film presented network chains; however, the fracture phenomenon was obvious. The width of the single chain was about 100 nm.

### 3.3. Uv-Vis spectral analysis

Figure 8 shows the Uv-Vis absorption spectrum of the  $\text{TiO}_2$  thin films with different coating numbers. The present experimental results show that the light absorption of the T-11 film was stronger under 550 nm illumination, according to the Scherer equation  $\lambda = 1240/E_g$  ( $\lambda$  was the limiting wavelength,  $E_g$  was the band gap energy); the band gap

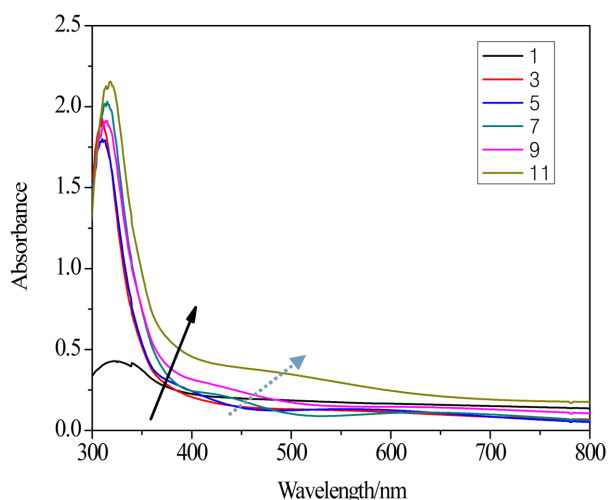


Fig. 8. Uv-Vis absorption spectra of  $\text{TiO}_2$  thin film with different coating numbers.

energy was 2.33 eV, which is far less than the value of 3.2 eV from the literature for pure  $\text{TiO}_2$ . The redshift degree was larger. The T-11 film was transparent; it has good light transmittance. The present experimental results show that the red shift becomes broader with increasing of the number of layers, while the increase of the number of layers is not good for the preparation of  $\text{TiO}_2$  thin films. We will further study the law of absorbance of a maximum level of light by increasing the number of layers. Diethanolamine as a surfactant to improve the uniformity of the film was beneficial to reduce the occurrence of reunions; it also improved the film transmittance and the specific surface area.

Figure 9 shows the Uv-Vis absorption spectra of the  $\text{BiVO}_4$  thin film with different incoating numbers. It can be seen that the  $\text{BiVO}_4$  film had a very strong absorption at 400-500 nm. The edge of the absorption band was at around 570 nm, according to the Scherer equation  $\lambda = 1240/E_g$  ( $\lambda$  was the limiting wavelength,  $E_g$  was the band gap energy); the band gap energy was 2.17 eV, which shows that the material had catalytic activity under visible light. The light absorption of the  $\text{BiVO}_4$  thin film coating was measured 3 and 4 times for all wavelengths and was found to be stronger than that of the  $\text{BiVO}_4$  thin film coating for the 1, 2 and  $\text{TiO}_2$  thin films. Moreover, the increase of the number of layers is still not good for the preparation of  $\text{BiVO}_4$  thin films.

Figure 10 provides a comparison chart for the Uv-Vis absorption spectra of B-3, the T-11 film and the  $\text{TiO}_2/\text{BiVO}_4$  layered film. It shows that all films have strong absorption in the UV region. In the visible region, the strongest absorption was found for the  $\text{BiVO}_4$  film; the  $\text{TiO}_2/\text{BiVO}_4$  layered films follow this and had values that were stronger than those of the T-11 film. The absorption band edge of the  $\text{TiO}_2/\text{BiVO}_4$  layered film showed redshift phenomenon, perhaps due to the Bi doped into the  $\text{TiO}_2$  lattice. On the other hand, the absorption to visible light of the  $\text{TiO}_2/\text{BiVO}_4$  layered film was weaker than that of pure  $\text{BiVO}_4$ , which may also be

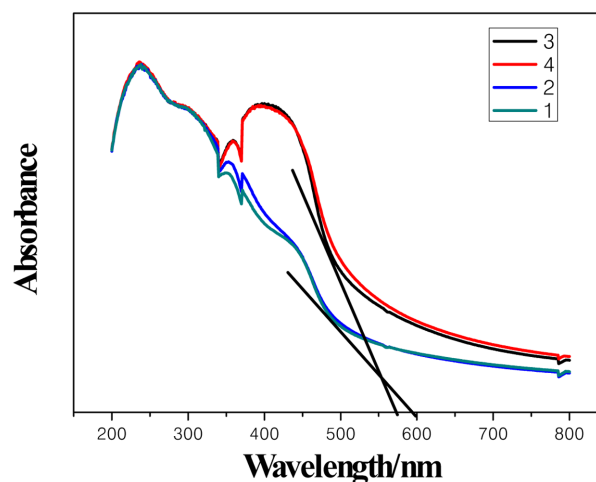


Fig. 9. Uv-Vis absorption spectra of  $\text{BiVO}_4$  thin film with different coating numbers.

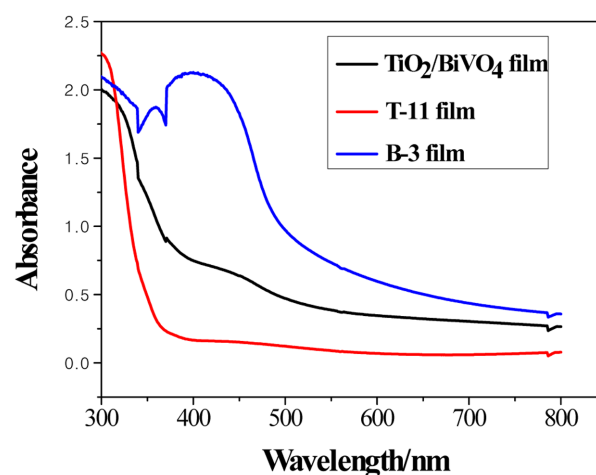
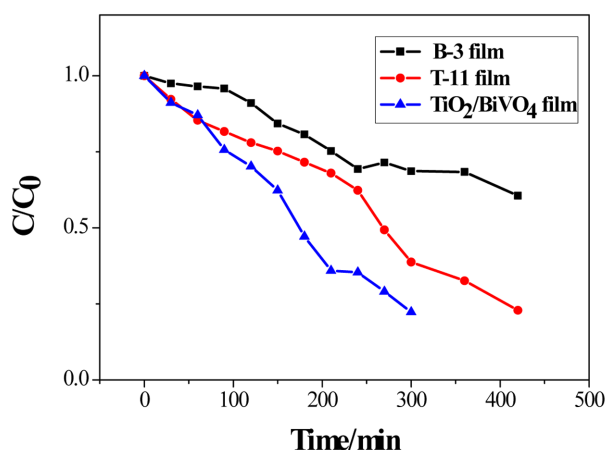


Fig. 10. Uv-Vis absorption spectra of T-11 thin film, B-3 thin film and  $\text{TiO}_2/\text{BiVO}_4$  thin film.

attributed to the presence of  $\text{TiO}_2$  thin film, which reduces the absorption of visible light by the composite film.

### 3.4. Degradation of methylene blue

Figure 11 provides a comparison chart for B-3, the T-11 film and the  $\text{TiO}_2/\text{BiVO}_4$  layered film degraded by methylene blue under visible light irradiation. The ability to degrade methylene blue solution of  $\text{TiO}_2/\text{BiVO}_4$  in a visible layered film was stronger than that of the pure B-3 film or the T-11 film. The rate of degradation of the  $\text{TiO}_2/\text{BiVO}_4$  layered film reached about 80% after 300 min, while that of the B-3 film was about 30% and that of the T-11 film was about 60%. When the time reached 420 min, the rate of degradation of the B-3 film was 40%; that of the T-11 film was about 80%. As is well known, the  $E_g$  potential is possibly a defect that can favor facile charge transfer. Therefore, the photocatalytic activity of the  $\text{TiO}_2/\text{BiVO}_4$  layered film cannot be higher than that of pure  $\text{BiVO}_4$ . However, by controlling the components, certain layers of  $\text{TiO}_2/\text{BiVO}_4$  can show higher



**Fig. 11.** Degradation curve of MB using B-3/T-11 and  $\text{TiO}_2/\text{BiVO}_4$  thin films under 550 nm irradiation.

photocatalytic activity than that of  $\text{TiO}_2$  or  $\text{BiVO}_4$  alone. Therefore, the catalytic activity under visible light of the  $\text{TiO}_2/\text{BiVO}_4$  layered film was much stronger than that of the single B-3 film or that of the T-11 film.

#### 4. Conclusions

A  $\text{TiO}_2/\text{BiVO}_4$  layered film containing anatase  $\text{TiO}_2$  and monoclinic phase  $\text{BiVO}_4$  was prepared. The  $\text{BiVO}_4$  film presented network chains, but a fracture phenomenon was obvious and the width of a single chain was about 100 nm. The absorption of the  $\text{TiO}_2/\text{BiVO}_4$  layered film in the visible light region was weaker than that of the  $\text{BiVO}_4$  film and better than that of the  $\text{TiO}_2$  thin film. The ability to degrade methylene blue solution of the  $\text{TiO}_2/\text{BiVO}_4$  layered film under visible light was stronger than that of the pure B-3 film or that of the T-11 film. The rate of degradation of the  $\text{TiO}_2/\text{BiVO}_4$  layered film reached about 80% after 300 min, while the B-3 film showed a value of about 30% and the T-11 film showed a value of about 60%.

#### Acknowledgments

This work was financially supported by the Natural Science Foundation of Anhui Education (KJ2015A026), Natural Science Foundation of Anhui Province (1408085MB33), the Science and Technology project of Anhui Province (1604a0802113), the Innovation Team Building Project of the Anhui University Research Platform (2016-2018) and

the College Students' Science and Technology Innovation Foundation (2016).

#### REFERENCES

1. P. Evana. P, M. E. Pemble, and D. W. Sheel, "Precursor-Directed Control of Crystalline Type in Atmospheric Pressure CVD Growth of  $\text{TiO}_2$  on Stainless Steel," *Chem. Mater.*, **18** 5750-55 (2006).
2. A. Fujishima, "Electrochemical Photolysis of Water at a Semiconductor Electrode," *Nature*, **238** 37-8 (1972).
3. Y. F. Gao, M. Nagai, and W. S. Seo, "Template-Freeself-Assembly of a Nanoporous  $\text{TiO}_2$  Thin Film," *J. Am. Ceram. Soc.*, **90** [3] 831 (2007).
4. M. Sidheswaran and L. L. Tavlarides, "Visible Light photocatalytic Oxidation of Toluene Using a Cerium-Doped Titania Catalyst," *Ind. Eng. Chem. Res.*, **47** 3346-57 (2008).
5. M. A. Khan, D. H. Han, and O. B. Yang, "Enhanced Photoresponse towards Visible Light in Ru-doped Titania Nanotube," *Appl. Surf. Sci.*, **255** 3687-90 (2009).
6. V. Stengl, S. Bakardjieva, and N. Murafa, "Preparation and Photocatalytic Activity of Rare Earth Doped  $\text{TiO}_2$  Nanoparticles," *Mater. Chem. Phys.*, **114** [1] 217-26 (2009).
7. R. Wang, "Light-Induced Amphiphilic Surfaces," *Nature*, **388** 431-32 (1997).
8. S. Jun, Z. Y. Xie, and X. X. Wu, "Sol-Gel Derived  $\text{SiO}_2$  Antireflective (AR) Coating Used in Solar Cells," *Rare Met. Mater. Eng.*, **37** [2] 47-50 (2008).
9. A. Kudo, K. Ueda, and H. Kato, "Photocatalytic  $\text{O}_2$  Evolution under Visible Light Irradiation on  $\text{BiVO}_4$  in Aqueous  $\text{AgNO}_3$  Solution," *Catal. Lett.*, **53** 229-30 (1998).
10. L. Zhang, D. Chen, and X. Jiao, "Monoclinic Structured  $\text{BiVO}_4$  Nanosheets: Hydrothermal Preparation, Formation Mechanism, and Coloristic and Photocatalytic Properties," *J. Phys. Chem. B*, **110** [6] 2668-73 (2006).
11. K. Akihiko, O. Keiko, and K. Hideki, "A Novel Aqueous Process for Preparation of Cyrsatl Fomr-Controlled and Highly Cyrsatlline  $\text{BiVO}_4$  Powder from Layered Vanadates at Room Temperature and Its Photocatalytic and Photophysical Properties," *Am. Chem. Soc.*, **121** [11] 459-67 (1999).
12. G. Li, "Synthesis and Photocatalytic Properties of  $\text{TiO}_2/\text{BiVO}_4$  Photocatalyst by Microwave-Assisted Hydrothermal Method," *Appl. Chem. Ind.*, **41** [2] 259 (2012).
13. H. Lei, "Preparation of  $\text{BiVO}_4/\text{TiO}_2$  Composite Photocatalyst and the Photocatalytic Degradation of Sodium Humate," *J. Mol. Catal.*, **27** [4] 377 (2013).
14. S. Y. Zhang, "Study on Preparation and Photocatalytic Properties of Mica-Loaded  $\text{TiO}_2/\text{BiVO}_4$  Composite Photocatalyst," *New Chem. Mater.*, **40** [10] 21 (2012).